Modelling of Cell Transport and Adhesion inside Porous Media

Shaun Johnston, Dr. Frantisek Stepanek.
Department of Chemical Engineering, Imperial College London, South Kensington Campus, London, UK.

Introduction

Tissue engineering involves growing living tissue or bone either in a bioreactor (in vitro) or in the body (in vivo). In vitro, the process begins with the fabrication of a scaffold into which cells are seeded. A constant supply of nutrients is then needed to enable growth of a cell culture and development of the required tissue or bone before transplantation into the patient's body. Figure 1 shows the main steps of tissue engineering; *Scaffold fabrication* involves the creation of the scaffold which the tissue will grow on. *Cell seeding* involves the introduction of cells onto the scaffold. This can be performed during the scaffold fabrication in some special cases. *Tissue growth* is the cultivating of the tissue, including the proliferation, migration, and differentiation of the cells through the porous scaffold. *Tissue transplantation* is the last step where the tissue is transplanted into the patient's body. This study concentrates on optimisation of scaffold design to assist cell seeding.

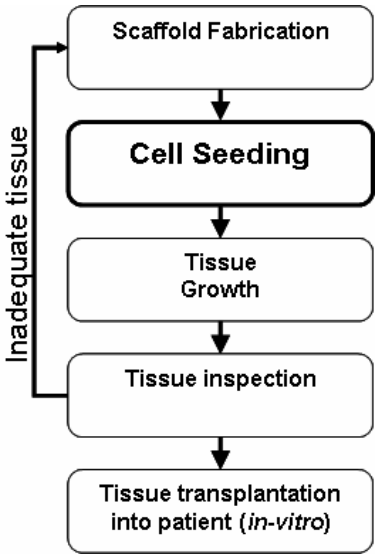

Figure 1, basic stages in the tissue engineering process.

The process of tissue engineering is currently largely empirical based. This has an obvious downfall in that it is both cost and time ineffective. The purpose of this paper is to construct a mathematical model which will enable simulation of the cell seeding process into porous media and provide a theoretical tool for use in tissue engineering. This should decrease the experimental iterations needed, Figure 1, reducing the demand on expensive resources and time associated with the area.

Method

The computational methodology is outlined in Figure 2; Firstly, geometries based on common tissue engineering scaffold fabrication techniques for making porous media are to be simulated, followed by detailed calculation of fluid velocity field and then the introduction of cells into the scaffold. To do this certain assumptions and techniques had to be developed in order to minimise computational time whilst ensuring reliability of results.

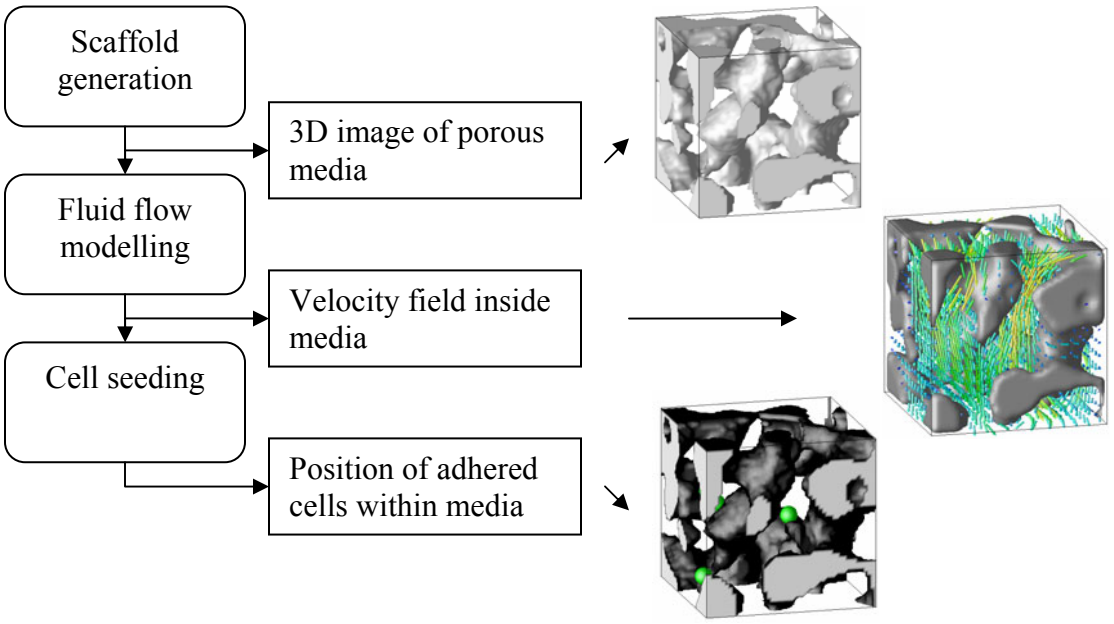

Figure 2, simulation progression from the initial scaffold geometry through to a cell seeded porous geometry; right-hand shows pictures of example simulations for each stage.

Scaffold generation

Geometries similar in morphology to scaffolds made by a co-continuous blend of two polymers have been generated using a Gaussian field technique (Adler and Thovert, 1998). The created geometries are represented by a 3D cubic array of 100 nodes for which a solid space is represented by a value of 1 and an empty space by a value of 0. A spatially correlated random field $Y(\underline{r})$ is generated from a field of independent normally distributed random variables $X(r)$ by the application of a linear filter.

$$Y(\underline{r}) = \sum_{\underline{s}} X(\underline{r}+\underline{s}) e^{-\left(\frac{\underline{s}}{\underline{L^*}}\right)^2} \qquad \textbf{(1)}$$

Where L^* is the correlation length.

Fluid flow simulations

The fluid flow program uses finite volume method (Kohout et al., 2005) for the solution of the Stokes equations (Equations 2-5) to calculate fluid velocities within a porous media. The Stokes' equations are considered since the cell seeding is typically done under conditions of low Reynolds numbers.

$$\nabla^2 p = 0 \quad \textbf{(2)}$$

$$\nabla^2 \underline{v}_{f\,i} = \frac{1}{\eta}\frac{\partial p}{\partial x_i} \quad \textbf{(3)}$$

Where i = 1, 2, 3

$$\int_0^v \int \underline{v}_{f\,3}\, dx_1 dx_2 = \dot{V} \quad \textbf{(4)}$$

$\underline{v}_f = 0$, at wall surface **(5)**

Where: $\underline{v}_{f3}$ is the velocity in the x_3 direction, p the pressure, x_i the distance along an axis 1, 2 or 3 and $\dot{V}$ the volumetric flow rate.

Cell seeding model

The cell seeding program introduces a number of cells one at a time at a user defined point in the porous scaffold along the z-axis (x_3). In our simulations 200 cells have been introduced to the scaffold at random positions $\underline{x}_i(0)$ across the x_1 and x_2 axis and at a position x_3=0.05. Cells, represented as spheres, travel down the fluid streamlines until they either leave the control volume at x_3=1 or attach to the scaffold wall.

Newton's law of motion, Equations 6 and 7, is used in conjunction with Stokes' Law to calculate the hydrodynamic drag on a cell and track its trajectory through the porous media.

$$\frac{d\underline{x}_i}{dt} = \underline{v}_s \quad \textbf{(6)}$$

$$\underline{v}_s(t+dt) = \underline{v}_s(t) + \frac{\underline{F}}{m}\cdot dt \quad \textbf{(7)}$$

Where t is time, $\underline{v}_s$ the velocity of the sphere, m the mass of the sphere, and $\underline{F}$ the drag force derived from equation 8.

$$\underline{F} = 6\cdot\pi\cdot r\cdot\eta\cdot\left(\underline{v}_f - \underline{v}_s\right) \quad \textbf{(8)}$$

Stokes' Law

Where, r is the radius of the sphere.

After a collision with a solid wall or another cell, a cell adheres if the cell adhesion force is larger than the force on the cell calculated from equation 8 with $\underline{v}_s = 0$, otherwise the cell carries on in the direction of its collision reflection vector.

Results from simulations will be presented in a dimensionless form. This allows the results to be scaled to whatever dimensions are needed within the assumed Reynolds Number of < 0.1.(Massey, 1998) The three main dimensionless variables are r^*, F^*_{adh} and ψ, where:

$$\psi = \frac{9}{2}\frac{\eta\tau}{\rho h^2} \quad \textbf{(9)}$$

$$F^*_{adh} = F_{adh}\frac{\tau}{6\pi\eta h^2} \quad \textbf{(10)}$$

$$r^* = \frac{r}{h} \quad \textbf{(11)}$$

Where h is the size of one voxel in the model.

After the model is transformed into dimensionless units the following parameters are then investigated in simulations:

- r^* The cell radius
- F^*_{adh} A force relating to cell-wall adhesion

With the following variables kept constant:

- ψ A value relating to viscous effect/inertial effect,
- The porosity, ε, and correlation length, L*, of the porous media
- The number of cells added to the system
- The initial position of added cells along the z axis

Simulation results

Simulations results were obtained investigating the effect of the cell-pore surface adhesion force and the size of cell radius on the number of cells adhered and their dispersion through the aforementioned porous media geometries. The results from 3 simulations were averaged where each simulation involved introducing 200 cells into the fluid field.

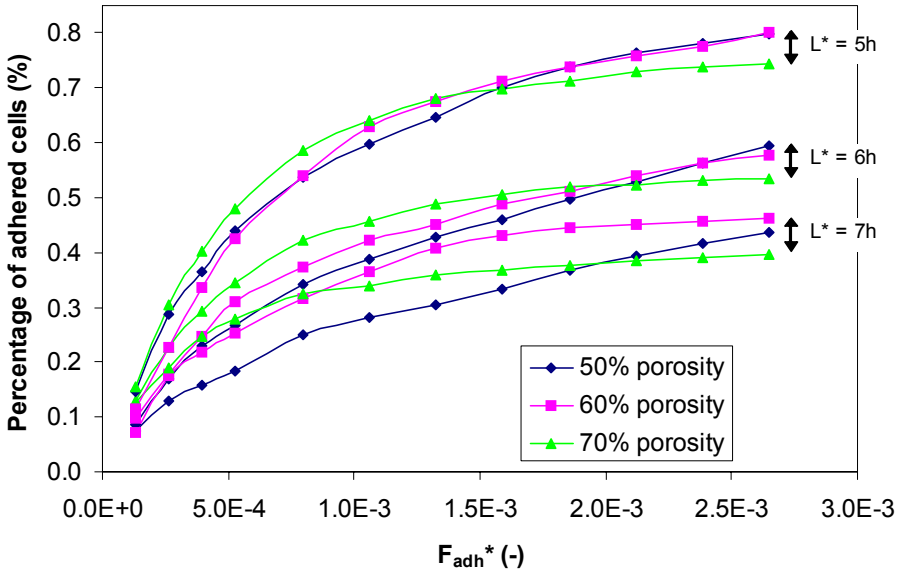

Figure 3, graph of cells adhered versus cell adhesion force, F_{adh}.

Figure 3 shows expected trends as an increase in cell adhesion force increases the number of cells adhering inside the porous geometry. Also evident is the negative effect the correlation length, L*, has on the number of cells adhering when the effect of porosity is almost negligible.

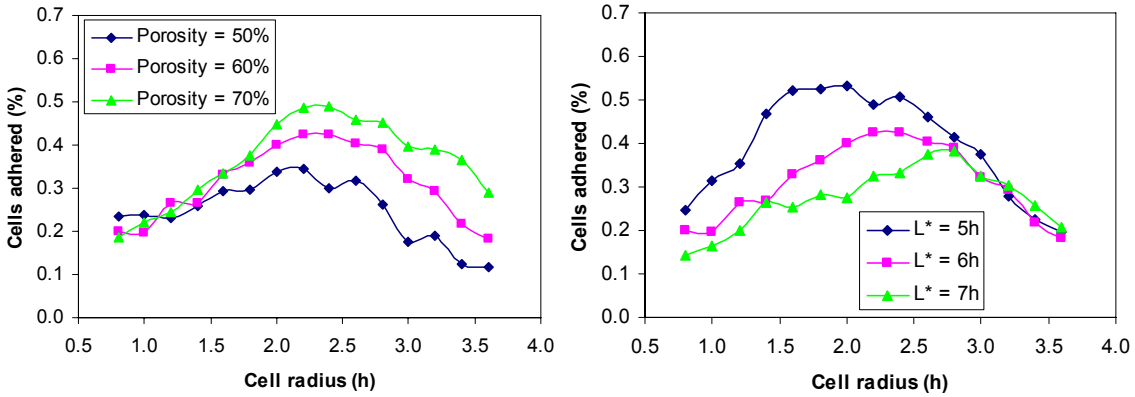

Figure 4, graphs of cells adhered versus cell radius, L* = 6(left) porosity = 60%(right).

Cell radius simulations show how an optimum cell size can be found for maximum cell retention inside the geometry, Figure 4. The effect of increasing a cells size will increase the cells momentum whilst also affecting the cell size to pore size ratio. It is evident from the effect of changing L* in Figure 3 together with the results in Figure 4 however that the cell size to pore size ratio alone has a large affect on the number of cells adhering.

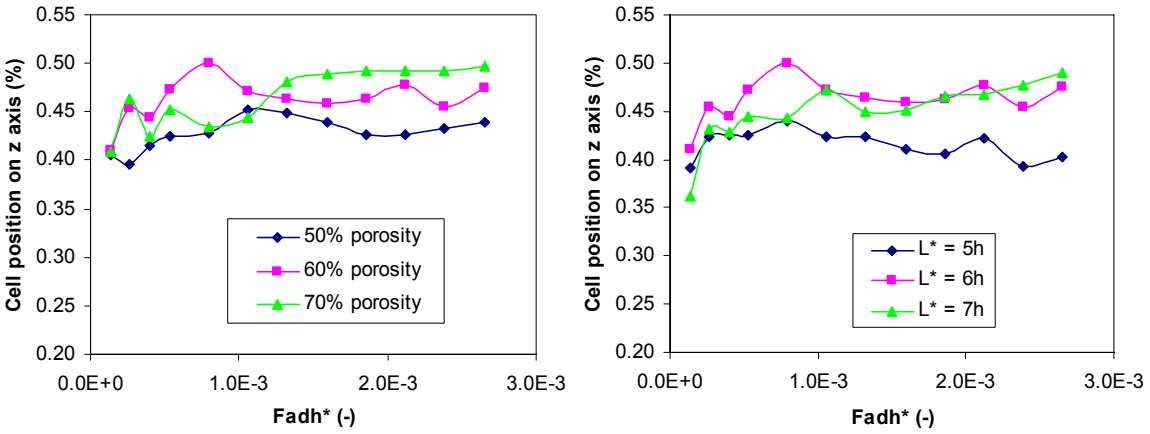

Figure 5, graphs of adhered cell position versus cell adhesion force, F_{adh}, L* = 6(left) porosity = 60%(right).

The cell adhesion force has little affect on where cells adhere through the scaffold geometry, as can be from Figure 5, whilst Figure 6 shows a clear negative correlation between the cell radius and position a cell has adhered inside the geometry. At a large cell radius it can be seen cells have adhered nearer the inlet of the geometry, but when cells are smaller a z axis position of 50%, which implies evenly dispersed cells is acquired.

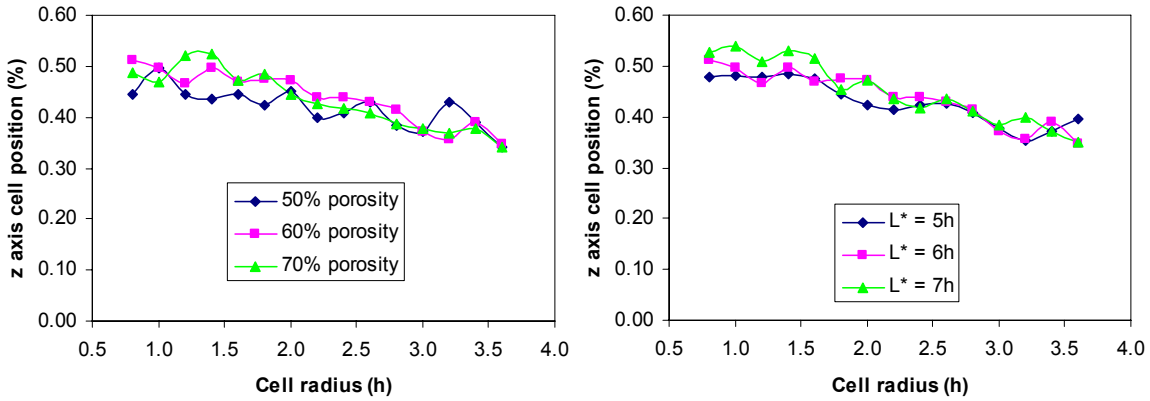

Figure 4, graphs of adhered cell position versus cell radius, L* = 6(left) porosity = 60%(right).

Conclusion

Results from simulations show that of the two variables tested, adhesion force and cell size, both affect the percentage of cells attached inside a porous structure, however only the cell size significantly controls the z-axis position of adhered cells inside the media.

It is also evident that a larger correlation length leads to more evenly distributed cells. This indicates that it is not necessarily the difference in momentum that a cell carries when the size of a cell changes but that the

physical size alone helps determine the distribution of cells throughout the scaffold. Hence the pore size in a tissue engineering scaffold could be used as a control in distributing cells in the cell seeding process.

Due to the adhesion force solely affecting the number of cells adhered inside the geometry it should therefore be possible to control both the cells adhered (cell density) and position of cells (cell dispersion) in a tissue engineering scaffold through use of only the perfusion rate through the scaffold and the scaffolds pore size.

The paper outlines a set of programs which are capable of predicting the affects of internal structure of a scaffold, cell size, cell-wall adhesion force and the fluid velocity field on the cell seeding process.

Acknowledgements

Financial support from the UK Engineering and Physical Sciences Research Council (EPSRC).

References

1. Adler,P.M. and Thovert,J.F., 1998. Real porous media: Local geometry and macroscopic properties. Appl. Mech. Rev., 51(9): 537-585.

2. Kohout,M., Collier,A.P., and Stepanek,F., 2005. Microstructure and transport properties of wet poly-disperse particle assemblies. Powder Technology, 156(2-3): 120-128.

3. Massey, B., 1998. Laminar flow between solid boundaries. In: Mechanics of Fluids. Stanley Thornes, pp. 204-260.